Nakayama, Shogo Nishi, Hatsue Ishibashi-Ueda, Atsushi Ohtaka, Yoshihiro Okamoto, Yasushi Nemoto.	Covered Stents: Geometrical Design of the Luminal Surface.	Organs			
Mariko Umeda, Mariko Harada-Shiba, Kingo Uchida, Yasuhide Nakayama	Photo-control of the Polyplexes Formation between DNA and Photo-cation Generatable Water-soluble Polymers.	Curr Drug Deliver		in press	2005
Yasuhide Nakayama, Takehisa Matsuda	Photocycloaddition-induced Preparation of Cyclic Macromolecules Using Biscinnamated or Biscoumarinated Oligo(ethylene glycol)s.	J Polym Sci Part A: Polym Chem		in press	2005
Haiying Huang, Yasuhide Nakayama, Kairong Qin, Kimiko Yamamoto, Joji Ando, Jun K Yamashita, Itoh Hiroshi, Keiichi Kanda, Hitoshi Yaku, Yoshihiro Okamoto, Yasushi Nemoto	In Vitro Pulsatile Flow Loading Can Induce the Differentiation from Embryonic Stem (ES) Cells to Vascular Wall Cells.	J Artif Organs		in press	2005
Osamu Sakai, Yasuhide Nakayama, Yasushi Nemoto, Yoshihiro Okamoto, Taiji Watanabe, Keiichi Kanda, Hitoshi Yaku	Development of Sutureless Vascular Connecting System for Easy Implantation of Small Caliber Artificial Grafts.	J Artif Organs		in press	2005
Ohtaka Atsushi,	Enhancement of Visible	Photochem		in press	2005

Takahiro Kameo, Yoshiaki Hirano, Yasuhide Nakayama	Light-Induced Gelation of Photocurable Gelatin by Addition of Polymeric Amine.	Photobiol			
中山泰秀	光反応によるバイオマテリアル界面の精密創製	ナノバイオエンジニアリング	2	19-29	2004
Hatsue Ishibashi-Ueda, Yasuhide Nakayama	Biotube technology for a novel tissue-engineered blood vessels.	Cardiovascular Regeneration Therapies using Tissue Engineering Approach		95-104	2005

雑誌（仁藤新治）

近藤靖、鈴木豊、仁藤新治	ヒト胚性幹細胞（ES 細胞）	バイオインダストリー	2	10-16	2005
N. Suzuki, R. Ikeda, M. S Kurokawa, S. Chiba, H. Yoshikawa, M. Ide, M. Tadokoro, S. Nito, N. Nakatsuji, Y. Kondo, K. Nagata, T. Hashimoto, Y. Ueda, E. Takada, C. Masuda.	Transplantation of Neural Cells derived from Retinoic Acid-treated Cynomolgus Monkey Embryonic Stem Cells successfully improved Motor Function of Hemiplegic Mice with Experimental Brain injury.	Neurobiology of Disease		in press	2005

Available online at www.sciencedirect.com

SCIENCE DIRECT

European Journal of Pharmacology 508 (2005) 255–265

www.elsevier.com/locate/ejphar

Therapeutic potential of thiazolidinediones in activation of peroxisome proliferator-activated receptor γ for monocyte recruitment and endothelial regeneration

Tokuji Tanaka[1], Yasutomo Fukunaga[1], Hiroshi Itoh*, Kentaro Doi, Jun Yamashita, Tae-Hwa Chun, Mayumi Inoue, Ken Masatsugu, Takatoshi Saito, Naoki Sawada, Satsuki Sakaguchi, Hiroshi Arai, Kazuwa Nakao

Department of Medicine and Clinical Science, Kyoto University Graduate School of Medicine, 54 Shogoin Kawahara-cho, Sakyo-ku, Kyoto 606-8507, Japan

Received 8 July 2004; received in revised form 18 October 2004; accepted 28 October 2004
Available online 30 December 2004

Abstract

Thiazolidinediones, a new class of antidiabetic drugs that increase insulin sensitivity, have been shown to be ligands for peroxisome proliferator-activated receptor γ (PPARγ). Recent studies demonstrating that PPARγ occurs in macrophages have focused attention on its role in macrophage functions. In this study, we investigated the effect of thiazolidinediones on monocyte proliferation and migration in vitro and the mechanisms involved. In addition, we examined the therapeutic potentials of thiazolidinediones for injured atherosclerotic lesions. Troglitazone and pioglitazone, the two thiazolidinediones, as well as 15-deoxy-Δ12,14-prostaglandin J2 inhibited in a dose-dependent manner the serum-induced proliferation of THP-1 (human monocytic leukemia cells) and of U937 (human monoblastic leukemia cells), which permanently express PPARγ. These ligands for PPARγ also significantly inhibited migration of THP-1 induced by monocyte chemoattractant protein-1 (MCP-1). Troglitazone and 15-deoxy-Δ12,14-prostaglandin J2 significantly suppressed the mRNA expression of the MCP family-specific receptor CCR2 (chemokine CCR2 receptor) in THP-1 at the transcriptional level. Furthermore, troglitazone significantly inhibited MCP-1 binding to THP-1. Oral administration of troglitazone to Watanabe heritable hyperlipidemic (WHHL) rabbits after balloon injury suppressed acute recruitment of monocytes/macrophages and accelerated re-endothelialization. These results suggest that thiazolidinediones have therapeutic potential for the treatment of diabetic vascular complications.

Keywords: Thiazolidinedione; PPARγ; MCP-1; CCR2; Macrophage; Insulin resistance

1. Introduction

Recruitment of circulating monocytes and their proliferation and differentiation into macrophages are not only the central events for initiation and progression of atherosclerosis, but have also been recently recognized as crucial pathogenic events in both diabetic micro- and macroangiopathy. Monocyte chemoattractant protein (MCP)-1 is a member of the C-C branch (or β) of the chemokine family and a potent monocyte and lymphocyte chemoattractant, which is expressed abundantly in atherosclerosic lesions (Nelken et al., 1991). MCP-1 initiates signal transduction through binding to the chemokine CCR2 receptor (CCR2) (Charo et al., 1994). In a study of CCR2 knockout mice, markedly fewer macrophages were present in the aorta of CCR2−/−, apoE−/− double knockout mice than in that of apoE−/− mice (Boring et al., 1998). Moreover, an independent study demonstrated that MCP-1−/− mice, when crossed with LDL receptor−/− mice, had smaller lesions and a significant reduction of macrophages in the lesions (Gu et al., 1998). These findings indicate the direct role of MCP-1 and CCR2 in monocyte recruitment and atherosclerosis.

* Corresponding author. Tel.: +81 75 751 3170; fax: +81 75 771 9452.
E-mail address: hiito@kuhp.kyoto-u.ac.jp (H. Itoh).
[1] These two authors contributed equally to this work.

0014-2999/$ - see front matter © 2004 Elsevier B.V. All rights reserved.
doi:10.1016/j.ejphar.2004.10.056

Thiazolidinediones are a new class of antidiabetic agents that increase sensitivity to insulin (Nolan et al., 1994). Insulin resistance has been attracting attention as the common casual factor not only for diabetes mellitus but also for hypertension, hyperlipidemia and obesity, all of which are risk factors for atherosclerosis (DeFronzo and Ferrannini, 1991). Recently, thiazolidinediones have been shown to be the ligands for peroxisome proliferator-activated receptor γ (PPARγ), which is a member of the nuclear receptor superfamily of ligand-activated transcription factors and has been identified as the functional receptor in antidiabetic action of thiazolidinediones (Lehmann et al., 1995).

PPARγ and the retinoid X receptor contain a heterodimer to bind regulatory elements in the promoter region of a number of adipocyte-specific genes and stimulate transcription (Tontonoz et al., 1994). In a previous study, we cloned rat PPARγ and detected down-regulation of PPARγ mRNA by several cytokines (Tanaka et al., 1999). Recent studies have demonstrated that PPARγ is expressed in cells of monocyte/macrophage lineage (Ricote et al., 1998; Tontonoz et al., 1998), and that oxidized low density lipoprotein (oxLDL), which plays a central role in atherogenesis, can regulate PPARγ-dependent gene transcription (Nagy et al., 1998). We recently reported that oxLDL potentiates, through the activation of PPARγ, the expression of vascular endothelial growth factor (VEGF) in human endothelial cells and in monocytes/macrophages (Inoue et al., 2001). Another study demonstrated that the administration of troglitazone, one of the thiazolidinediones, to Watanabe heritable hyperlipidemia (WHHL) rabbits and high fat-fed low density lipoprotein receptor or apo E knockout mice inhibits progression of atherosclerosis (Shiomi et al., 1999; Chen et al., 2001; Collins et al., 2001). All of these studies indicate the significance of PPARγ in monocyte and macrophage functions and atherogenesis.

The objective of the study presented here was to determine the effect of thiazolidinediones on the migration and proliferation of monocytes/macrophages and to investigate the molecular mechanism of the effect of thiazolidinediones on MCP-1-induced monocyte migration, with the focus on the expression of CCR2. Furthermore, we used WHHL atherosclerotic rabbits for an in vivo investigation of the therapeutic potentials of thiazolidinediones for acute monocyte recruitment and infiltration as well as for endothelial regeneration after acute vascular injury.

2. Materials and methods

2.1. Cell culture

THP-1 (human monocytic leukemia cells) and U937 (human monoblastic leukemia cells) were obtained from ATCC and cultured as previously reported (Inoue et al., 2001), with or without the following agents: troglitazone (Sankyo, Tokyo, Japan), pioglitazone (Takeda Chemical Industries, Osaka, Japan), 15-deoxy-Δ12,14-prostaglandin J2 (Sigma, St. Louis, MO), which is one of the natural ligands of PPARγ, or 9-*cis*-retinoic acid (Sigma), which is the ligand of the retinoid X receptor.

2.2. Northern blot analysis

Total cellular RNA was isolated from cultured cells using TRIzol reagents (Gibco BRL, Gaithersburg, MD). Northern blot analysis was performed as described elsewhere (Tanaka et al., 1999). The human PPARγ probe consisted of an 858-base pair fragment of the cDNA corresponding to nucleotides 329–1186 of the human PPARγ1 cDNA. The human CCR2 probe consisted of a 939-base pair fragment of the CCR2 cDNA corresponding to nucleotides 1–939. A human β-actin probe (Wako, Japan) was used to monitor the amount of total RNA in each sample.

2.3. Establishment of U937 cells permanently expressing PPARγ

U937 cells permanently expressing PPARγ were established by using the PPARγ expression vector (pCMX-mPPARγ), which contains a cytomegalovirus enhancer and mouse full-length PPARγ cDNA, as we previously reported and explained in detail (Inoue et al., 2001).

2.4. Chemotaxis assay

The cell migration was evaluated with the modified Boyden chamber technique using a 96-well chemotaxis chamber (Neuroprobe, Cabin John, MD) with 50 μl of cell suspension (2×10^7 cells/ml cells in Roswell Park Memorial Institute medium (RPMI)), as previously reported by us (Sawada et al., 2000).

2.5. Equilibrium binding analysis

The cells were suspended at a density of 2×10^7 cells/ml in 200 μl of binding buffer containing 0.1% bovine serum albumin. The cells were incubated with 0.02 nM ^{125}I-MCP-1 and various amounts of unlabelled ligand for 90 min at 25 °C. All assays were done in triplicate, and binding data were examined with the Ligand Assistance Program (Ligand Pharmaceuticals, Charlotte, NC) or Scatchard analysis.

2.6. Balloon angioplasty and troglitazone administration

Homozygous male WHHL rabbits (10 months old, 3.6±0.1 kg) were used for this study. The rabbits were supplied by Sankyo Pharmaceutical. All animals used in the present study were treated with humane care in compliance with the *Guide for the Care and Use of Laboratory Animals* prepared by the National Academy of Sciences and published by the National Institutes of Health (NIH

publication No. 85-23, revised 1985). Each WHHL rabbit was fully anesthetized with sodium pentobarbital (25 mg/kg body weight). A 4F Fogarty balloon catheter was inserted from the left femoral artery, and after the balloon was inflated with air (0.3 ml in the thoracic region and 0.2 ml in the abdominal region), the intima of the thoracic and abdominal aorta was denuded by three passages of the catheter, as we previously reported (Doi et al., 2001). One group (n=8) received troglitazone at a concentration of 100 mg/kg body weight/day from 2 weeks before the angioplasty until 6 weeks after the balloon treatment and the other group (n=8) was given a control solvent. Two rabbits in the control group died during the catheterization and were dropped from the study.

2.7. Pathological examination, immunohistochemical analysis and evaluation of re-endothelialization

The rabbits were fully anesthetized and then killed 6 weeks after the angioplasty. Thirty minutes before they were killed, the animals received an intravenous injection of 6 mL of 0.5% Evans blue dye delivered via the ear vein to identify the remaining non-endothelialized area, as previously described by us (Doi et al., 2001). The area of the intimal surface that was stained blue after the application of Evans blue dye was considered to represent the portion of the arterial segment that remained endothelium deficient. Computerized planimetry (NIH image ver 1.61) was used for analysis. Next, two segments each from the thoracic aorta and the abdominal aorta were obtained from each rabbit (four sites per rabbit). The segments were fixed in methanol–Carnoy's fixative and processed routinely, embedded in paraffin and sectioned into 5-μm-thick slices. The serial sections from each segment were stained with hematoxylin–eosin or with the anti-smooth muscle actin monoclonal antibody (mAb) (1A4; Deckman) or with anti-rabbit macrophage mAb RAM11 (Dako), as we previously reported (Inoue et al., 1998). The acute recruitment or infiltration of macrophages after the angioplasty was evaluated by counting the number of RAM-11$^+$ macrophages on the surface of the aorta (see Fig. 6).

2.8. Reverse transcription-polymerase chain reaction (RT-PCR) for VEGF

The aorta was frozen in liquid N2 immediately after sacrifice and stored at −80 °C until further study. The frozen aorta was homogenized in cold TRIzol reagent (Invitrogen) and total RNA was extracted according to the manufacturer's instructions. cDNA synthesis was performed with 1 μg of total RNA, oligo(dT)20 and ThermoScript (Invitrogen). Incubation lasted for 40 min at 55 °C. The sense primer for rabbit VEGF was 5′GTGGACATCTT CCAGG AGTA-3′and the antisense primer 5′TCTTTGGTCTGCATTCAC A-3′as described previously (Skorjanc et al., 1998). For rabbit G3PDH, the sense primer was 5′ACCACGGTGCACGCCATCAC-3′ and the antisense primer was 5′TCCACCA CCCTGTTGCTGTA-3′ PCR was performed with 2 μL of cDNA template, 2.5U Platinum Taq DNA Polymerase (Invitrogen) and 0.4 μM of the sense and antisense primers. The annealing temperature was 57 °C for VEGF and 60 °C for G3PDH and the number of cycles was 30 for both. Product detection [226 nucleotides for VEGF and 450 for G3PDH] was performed after electrophoresis on 2% agarose gel using ethidium bromide staining.

2.9. Statistical analysis

All values were expressed as mean±S.E.M. Factorial analysis of variance (ANOVA) followed by the Fischer's protected least significant difference test was used to identify significant differences in multiple comparisons.

3. Results

3.1. Induction of PPARγ expression by PPARγ and retinoid X receptor ligands in monocytes/macrophages

PPARγ mRNA was not detected in U937 whether treated or not with PPARγ and retinoid X receptor ligands. While unstimulated THP-1 expressed PPARγ mRNA at a low level, treatment of THP-1 with PPARγ ligands (10^{-5} mol/l troglitazone, 10^{-5} mol/l pioglitazone, or 10^{-5} mol/l 15-deoxy-Δ12,14-prostaglandin J2) or retinoid X receptor ligand (10^{-7} mol/l 9-*cis*-retinoic acid) resulted in a significant increase of PPARγ expression in THP-1. Stimulation with a combination of troglitazone and 9-*cis*-retinoic acid resulted in further up-regulation of PPARγ mRNA expression (Fig. 1).

3.2. Inhibition of proliferation of THP-1 by PPARγ and retinoid X receptor ligands

Cells (1.0×10^5 cells/ml) were cultured for 5 days in the presence of various doses of one of the thiazolidinediones, 15-deoxy-Δ12,14-prostaglandin J2, 9-*cis*-retinoic acid or combination thereof. When cells were treated with vehicle alone, the number of cells significantly increased 7.2 times after 5 days in culture. Troglitazone, pioglitazone, 15-deoxy-Δ12,14-prostaglandin J2 or 9-*cis*-retinoic acid caused a concentration-dependent suppression of cell growth. With 10^{-5} mol/l troglitazone, pioglitazone, 15-deoxy-Δ12,14-prostaglandin J2 and 10^{-7} mol/l 9-*cis*-retinoic acid alone, cell proliferation was inhibited by 60%, 51%, 56% and 39%, respectively, after 5 days. The simultaneous treatment of cells with both 10^{-5} mol/l troglitazone and 10^{-7} mol/l 9-*cis*-retinoic acid produced a 77% inhibition of cell growth. No effect was observed with troglitazone (10^{-5} mol/l) when used alone or in combination with 9-*cis*-retinoic acid (10^{-7} mol/l) in U937 cells in which PPARγ was not detected.

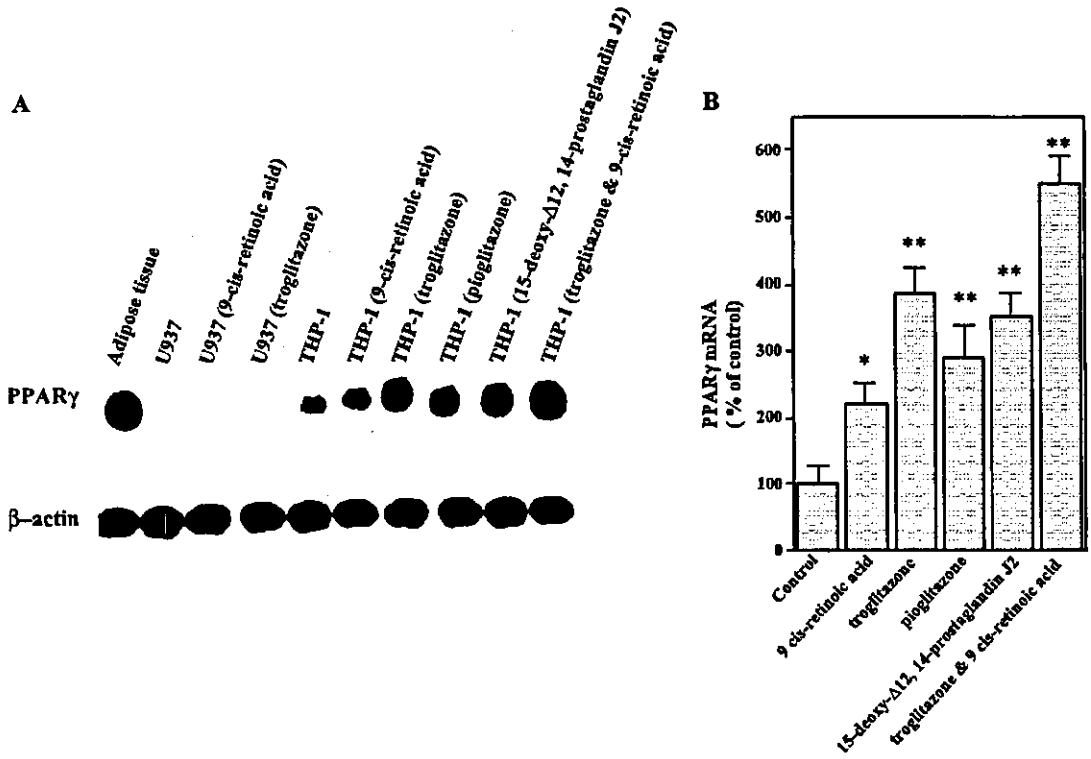

Fig. 1. Induction of PPARγ mRNA expression by PPARγ and retinoid X receptor ligands in monocytes/macrophages. U937 and THP-1 were incubated with 10^{-5} mol/l of troglitazone, pioglitazone, and 15-deoxy-Δ12,14-prostaglandin J2 and with 10^{-7} mol/l of 9-*cis*-retinoic acid for 24 h and their effects on PPARγ mRNA expression were evaluated by Northern blot analysis. (A) Northern blot analysis of PPARγ mRNA in adipose tissue, U937, and THP-1. Twenty micrograms of total RNA per lane were used for the analysis. (B) Quantitative measurements of PPARγ mRNA levels in THP-1. *P<0.05 and **P<0.01 vs. corresponding controls (n=4).

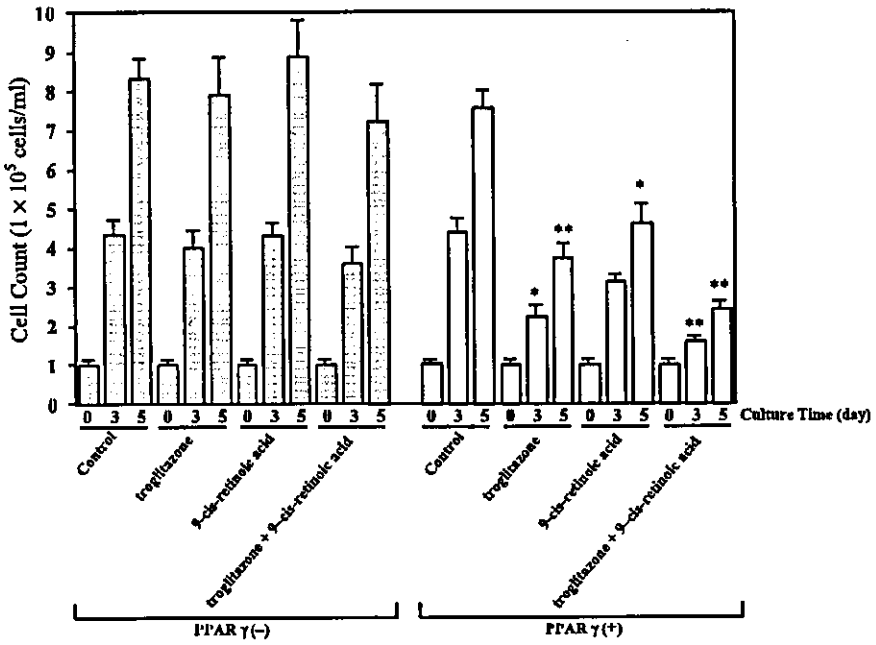

Fig. 2. Inhibition of proliferation of U937 cell expressing PPARγ by troglitazone and 9-*cis*-retinoic acid. Wild-type U937 cells and U937 cells stably transfected with PPARγ expression vector were plated at 1.0×10^5 cells/ml and cultured for 5 days in the presence of 10^{-5} mol/l of troglitazone and 10^{-7} mol/l of 9-*cis*-retinoic acid alone or in combination. Cell numbers were counted after 3 and 5 days. *P<0.05 and **P<0.01 vs. corresponding controls (n=4).

3.3. Restoration of responsiveness to troglitazone and 9-cis RA in U937 expressing PPARγ

To further characterize the role of PPARγ in monocytes/macrophages proliferation, we utilized the permanent cell line of U937 expressing PPARγ. As shown in Fig. 2, troglitazone or 9-*cis*-retinoic acid treatment of these cell lines resulted in a marked inhibition of cell growth, similar to that of THP-1. With 10^{-5} mol/l of troglitazone alone, cell proliferation was inhibited by 56% after 5 days, and with 10^{-7} mol/l 9-*cis*-retinoic acid alone by 45%. Moreover, treatment of the cells with a combination of 10^{-5} mol/l troglitazone and 10^{-7} mol/l 9-*cis*-retinoic acid resulted in a 71% inhibition of cell growth (Fig. 2).

3.4. Inhibition of MCP-1-induced migration of THP-1 by PPARγ and retinoic X receptor ligands

The chemotactic response of THP-1 to MCP-1, troglitazone, 15-deoxy-Δ12,14-prostaglandin J2 and 9-*cis*-retinoic acid was assessed during a 2-h incubation. The treatment with MCP-1 resulted in a dose-dependent induction in the migration of THP-1 (5 To 50 ng/ml), but THP-1 cells did not show a significant migratory response to troglitazone, 15-deoxy-Δ12,14-prostaglandin J2 or 9-*cis*-retinoic acid. Pretreatment with troglitazone for 24 h significantly inhibited the migration of THP-1 induced by MCP-1 (25 ng/ml), and with 10^{-7} mol/l troglitazone, the migration of THP-1 was inhibited by 44%. Maximal inhibition (66%, $P<0.01$) of THP-1 migration was observed in response to treatment with 10^{-4} mol/l troglitazone (Fig. 3A). Pretreatment with 15-deoxy-Δ12,14-prostaglandin J2 or 9-*cis*-retinoic acid also inhibited the migration of THP-1 under the same conditions (Fig. 3B,C), while troglitazone and 9-*cis*-retinoic acid (10^{-7} mol/l) had an even more profound inhibitory effect on migration (Fig. 3D).

3.5. Regulation of CCR2 mRNA expression by troglitazone, 15-deoxy-Δ12,14-prostaglandin J2 and 9-cis RA In THP-1

We also examined the effect of troglitazone, 15-deoxy-Δ12,14-prostaglandin J2 and 9-*cis*-retinoic acid on CCR2

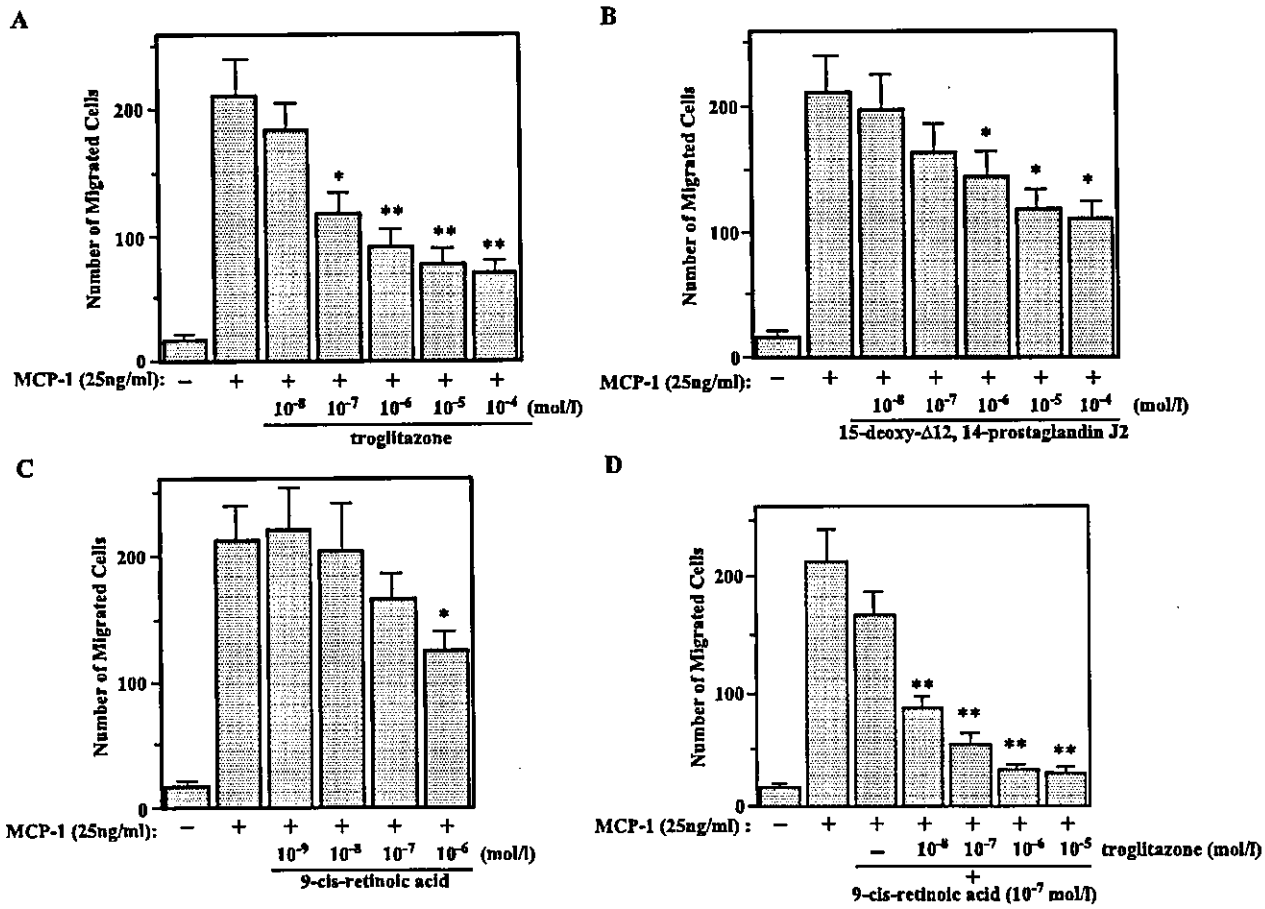

Fig. 3. Inhibition of MCP-1-induced migration of THP-1 by PPARγ and retinoid X receptor ligands. THP-1 were pretreated with different concentrations of troglitazone (A), 15-deoxy-Δ12,14-prostaglandin J2 (B), 9-*cis*-retinoic acid (C) alone or in combination with troglitazone and 9-*cis*-retinoic acid (D) for 24 h at 37 °C. MCP-1 (25 ng/ml) was added to the lower wells as the chemoattractant and 2 h migration assays were performed ($n=6$). *$P<0.05$ and **$P<0.01$ vs. 25 ng/ml of MCP-1 alone.

expression. treatment with 10^{-5} mol/l troglitazone resulted in a time-dependent reduction in the expression of CCR2 mRNA. The inhibitory effect of 10^{-5} mol/l of troglitazone was first observed after a 6-h incubation and persisted for at least a 48-h exposure (Fig. 4A). Treatment with troglitazone (10^{-7} mol/l to 10^{-4} mol/l) suppressed CCR2 mRNA expression in a dose-dependent fashion (Fig. 4B,C). The maximum decrease of 93% occurred in response to 10^{-4} mol/l of troglitazone. Treatment with 15-deoxy-Δ12,14-prostaglandin J2 (10^{-6}–10^{-4} mol/l) and with 9-*cis*-retinoic acid (10^{-7}–10^{-6} mol/l) also suppressed the CCR2 mRNA level in a dose-dependent fashion (Fig. 4B,C).

To determine whether the down-regulation of CCR2 is a transcriptional or post-transcriptional event, we analyzed the effect of troglitazone on the expression of CCR2 mRNA in the presence of actinomycin D (3 μg/ml, Sigma), a transcriptional inhibitor. When treated with actinomycin D, a linear decrease in the level of CCR2 mRNA without the treatment of troglitazone was observed (T1/2; 3 h). With the treatment of troglitazone, the level of CCR2 mRNA also

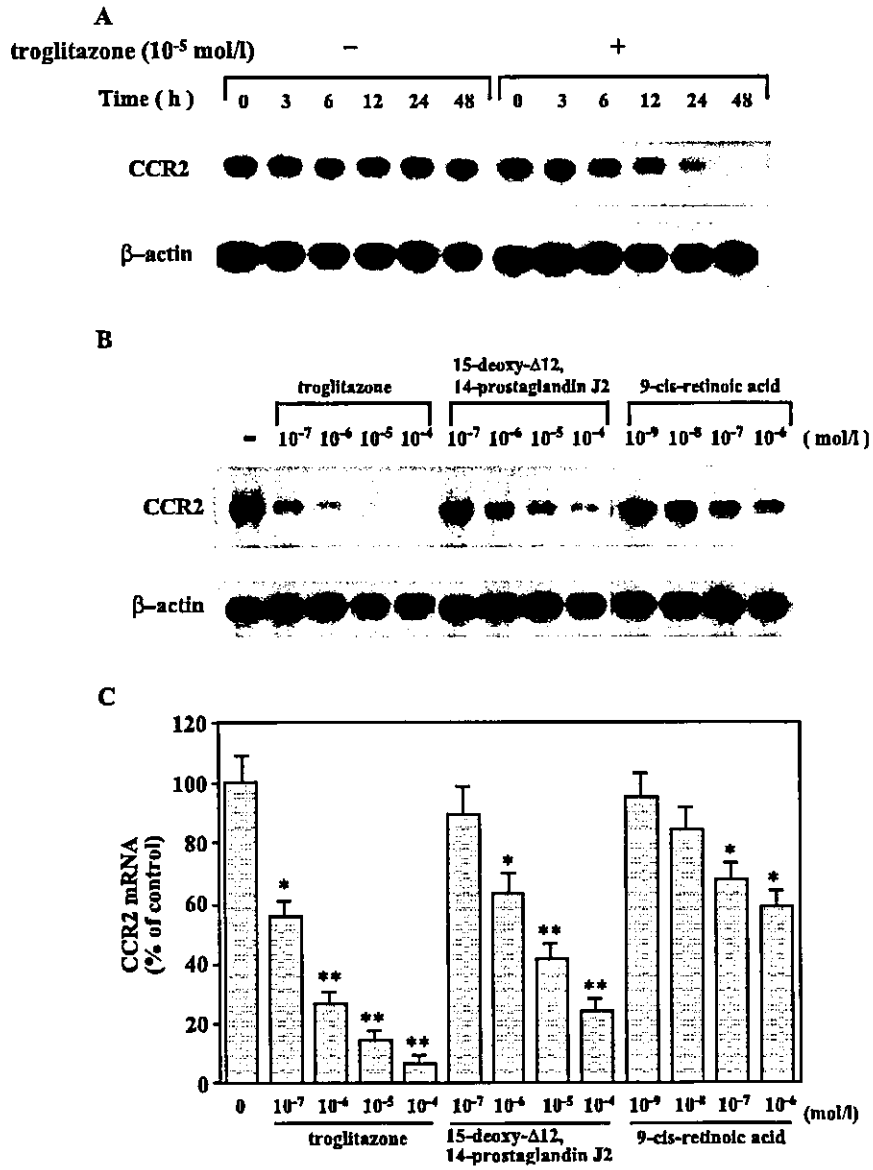

Fig. 4. Regulation of CCR2 mRNA expression by troglitazone, 15-deoxy-Δ12,14-prostaglandin J2 or 9-*cis*-retinoic acid in THP-1. (A) Time-dependent effect of troglitazone on CCR2 mRNA expression. THP-1 cells were incubated with or without 10^{-5} mol/l of troglitazone and harvested after various incubation times for RNA isolation. Twenty micrograms of total RNA per lane was used for the analysis. Similar results were obtained in three independent experiments. (B) Concentration-dependent effect of troglitazone, 15-deoxy-Δ12,14-prostaglandin J2 and 9-*cis*-retinoic acid on CCR2 mRNA expression. THP-1 were incubated with or without various concentrations of troglitazone, 15-deoxy-Δ12,14-prostaglandin J2 and 9-*cis*-retinoic acid harvested 24 h after incubation. Twenty micrograms of total RNA per lane was used for the analysis. (C) Quantitative measurements of CCR2 mRNA levels after administration of troglitazone, 15-deoxy-Δ12,14-prostaglandin J2, or 9-*cis*-retinoic acid. $^{*}P<0.05$ and $^{**}P<0.01$ vs. corresponding controls ($n=4$).

decreased, but at a similar rate to that of the control not treated with troglitazone (Fig. 5A,B).

3.6. Inhibition of MCP-1 binding to THP-1 by troglitazone and 9-cis RA

Under the same experimental condition as described above, we also examined the effects of troglitazone on the binding of MCP-1 to THP-1. THP-1 was pretreated for 24 h with or without 10^{-5} mol/l of troglitazone. As illustrated in Fig. 6A, Scatchard analysis showed that K_d values were similar for the control and troglitazone-treated groups (0.61±0.13 nmol/l for the control and 0.65±0.16 nmol/l for the troglitazone-treated group). In contrast, the troglitazone-treated THP-1 expressed 4.3±0.8 fmol of receptors/10^6 cells, while the control THP-1 expressed 11.7±1.6 fmol/10^6 cells. Thus, troglitazone (10^{-5} mol/l) reduced the number of MCP-1 receptor on the cell surface by 64%. Fig. 6B shows the time course of the effect of troglitazone and 9-*cis*-retinoic acid on the binding of MCP-1 to THP-1. At 10^{-5} mol/l of troglitazone alone, the binding was inhibited by 51% after 12 h and by 66% after 24 h, and the simultaneous treatment of cells with 10^{-5} mol/l troglitazone and 10^{-7} mol/l 9-*cis*-retinoic acid resulted in 85% inhibition.

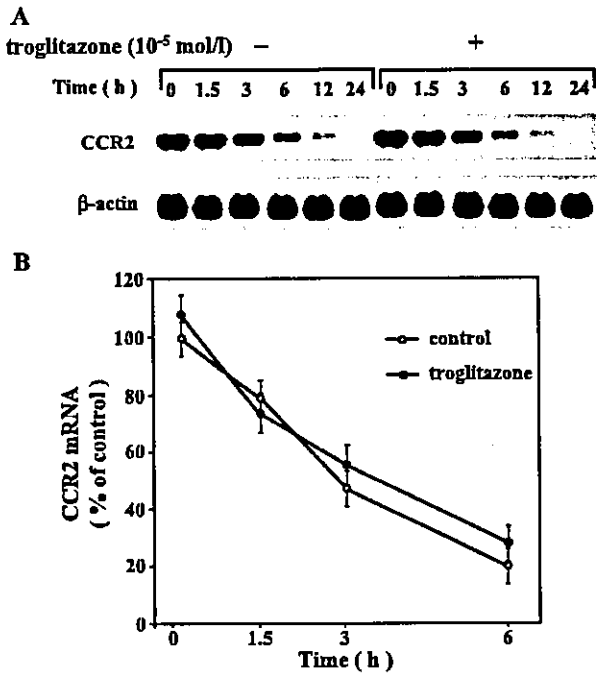

Fig. 5. Effect of troglitazone on the expression of CCR2 mRNA in the presence of actinomycin D. (A) THP-1 were incubated with 3 μg/ml of actinomycin D with or without 10^{-5} mol/l of troglitazone for 24 h and harvested after various incubation times for RNA isolation. Twenty micrograms of total RNA per lane was used for the analysis. (B) Quantitative measurements of CCR2 mRNA levels after treatment with 3 μg/ml of actinomycin D with or without 10^{-5} mol/l of troglitazone (n=3).

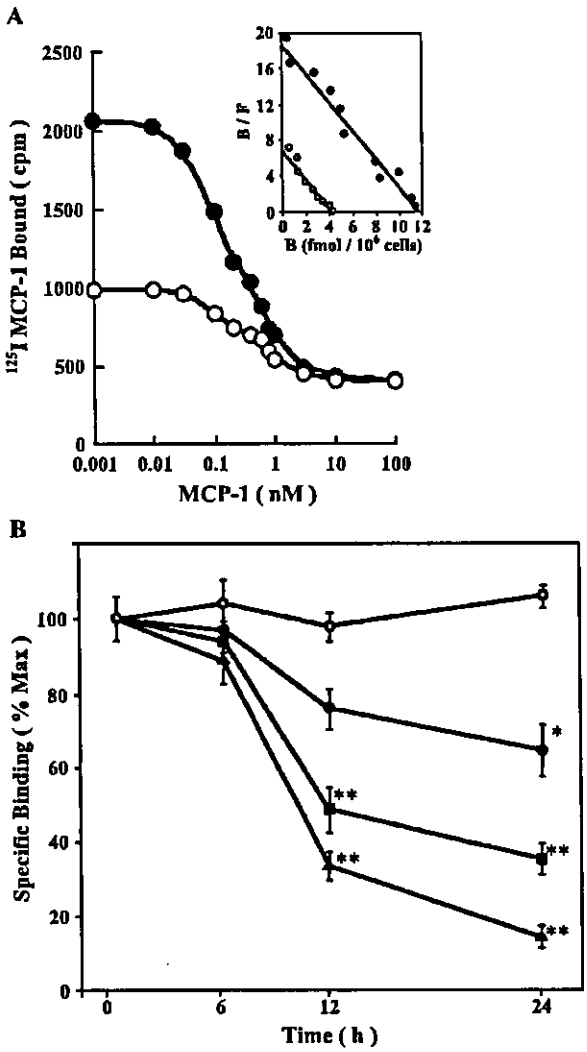

Fig. 6. Inhibition of MCP-1 binding to THP-1 by troglitazone and 9-*cis*-retinoic acid. (A) ^{125}I-labelled MCP-1 binding curve and Scatchard plot analysis. THP-1 were pretreated with (white circles) or without (black circles) 10^{-5} mol/l of troglitazone for 24 h at 37 °C. Insets show Scatchard analysis of the specific binding data. The results are representative of three independent experiments. (B) Time course of troglitazone and 9-*cis*-retinoic acid-induced reduction of MCP-1 binding to THP-1. The cells were incubated for up to 24 h at 37 °C without treatment (white circle) or with 10^{-5} M of troglitazone (black square) or 10^{-7} mol/l of 9-*cis*-retinoic acid (black circle) alone or in combination (black triangle). The binding of ^{125}I-MCP-1 was determined in the presence or absence of 100 nmol/l of unlabeled MCP-1. *P<0.05 and **P<0.01 vs. corresponding controls.

3.7. Suppression by troglitazone of monocyte and macrophage recruitment onto the balloon-injured aorta of WHHL rabbits

At the end of the study, 10-month-old WHHL rabbits belonging to the control group exhibited severe atherosclerotic lesions in thoracic aortae (61±11% of the total surface area) and patchy lesions in abdominal aortae (37±9%). Treatment with troglitazone for a total of 8 weeks did not

noticeably change the gross appearance of the atherosclerotic lesions (66±8% in thoracic aortae and 32±7% in abdominal aortae). The immunohistochemical analysis showed that the troglitazone treatment had no significant effect on the total content of $1A4^+$ vascular smooth muscle cells (1A4-positive area/atheromatous area: 11.4±3.9% in

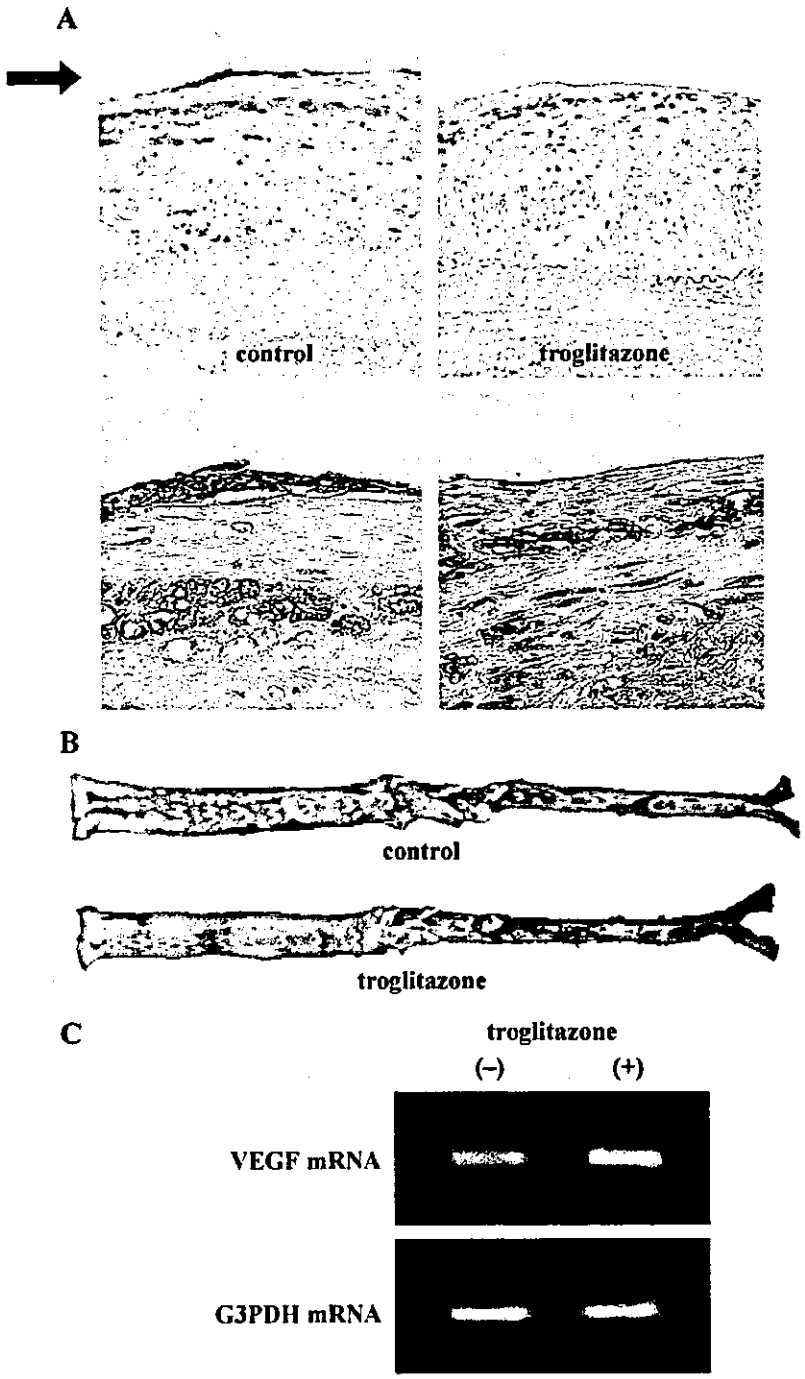

Fig. 7. Effect of troglitazone administration to balloon-injured WHHL rabbits. (A) Suppression of recruitment of monocytes/macrophages onto the surface of the aorta of WHHL rabbits 6 weeks after balloon injury. Troglitazone was administered every day for 8 weeks, from 2 weeks before injury until sampling. RAM11-positive immunostaining shows monocytes/macrophages in brown. Top: Lower magnification of the whole blood vessel. Bottom: Higher magnification of the surface of the balloon-injured aortas (the portion indicated by arrow in top). (B) Macroscopic appearance of balloon-injured aortas of WHHL rabbits after the injury. Area of re-endothelialization is not stained by Evans blue dye and appears white. Control: vehicle-treated group; troglitazone: troglitazone-treated group. (C) Analysis of VEGF gene expression. Pooled frozen aortic samples (vehicle-treated group: n=6; troglitazone-treated group: n=8) were subjected to RT-PCR for VEGF.

the abdominal and 9.3±1.1% in the thoracic aortae of the control group; 6.3±0.7% in the abdominal and 7.8±1.7% in the thoracic aortae of the troglitazone-treated group), although there was a tendency for the vascular smooth muscle cell content to decrease as a result of the troglitazone treatment, which is compatible with the results of previous studies with different experimental protocols (Shiomi et al., 1999; Law et al., 1996). Nor did the treatment significantly affect the total content of RAM11$^+$ monocytes/macrophages (RAM11-positive area/atheromatous area: 11.6±3.7% in the thoracic and 14.3±4.8% in the abdominal aortae of the control group; 14.9±3.1% in the thoracic and 12.8±2.5% in the abdominal aortae of the troglitazone-treated group).

However, the number of acutely recruited monocytes/macrophages onto the surface of the balloon injured aorta was significantly lower in the abdominal aorta of the troglitazone-treated group (39±5% of the control, $P<0.05$), although in the thoracic aorta of this group the reduction in numbers did not reach statistical significance (82±7% of the control) (Fig. 7A).

3.8. Re-endothelialization in balloon-injured aorta of WHHL rabbits accelerated by troglitazone

Evans blue staining demonstrated that the denuded area was significantly smaller in the aorta of the troglitazone-treated group than of the control group (Fig. 7B; Evans blue-stained area/non-atheromatous area: 0.4±0.2% for the troglitazone-treated and 4.8±1.2% for the control group; $P<0.05$). RT-PCR for VEGF showed that VEGF gene expression had increased in the aorta of the troglitazone-treated group (Fig. 7C).

4. Discussion

The study presented here demonstrated that PPARγ and retinoid X receptor ligands caused a concentration-dependent suppression of cell growth in PPARγ-expressing THP-1 cells. In contrast, troglitazone and 9-*cis*-retinoic acid had no effect on the proliferation of wild-type U937 which lack PPARγ expression. We further demonstrated that U937 cell lines with stable PPARγ expression restored the responsiveness to troglitazone and 9-*cis*-retinoic acid for growth suppression. These findings indicate that activation of PPARγ in monocytes/macrophages causes growth suppression of these cell lines.

We could also demonstrate that PPARγ and retinoid X receptor specific ligands strongly inhibited the MCP-1-induced migration of THP-1. This result is compatible with those reported in previous publications (Zhu et al., 1999; Kintscher et al., 2000). To investigate the potential mechanism of inhibition of MCP-1-induced migration by PPARγ activation, we also examined changes in the functional expression of CCR2 in THP-1. We found that troglitazone, 15-deoxy-Δ12,14-prostaglandin J2 and 9-*cis*-retinoic acid had a strong down-regulatory effect on CCR2 mRNA expression at the transcriptional level. We further confirmed that MCP-1 binding activity was also reduced and the number of MCP-1 receptors (CCR2) declined as a result of exposure to troglitazone and 9-*cis*-retinoic acid. Since it has been reported that in an in vitro chemotaxis assay, monocytes derived from CCR2 knockout mice failed to migrate in response to MCP-1 (Boring et al., 1997), the suppressive action of PPARγ and retinoid X receptor ligands on MCP-1-induced migration can be interpreted as representing the down-regulation of CCR2 expression.

Other studies have demonstrated that CCR2 or MCP-1 knockout mice are less susceptible to atherosclerosis and showed low monocyte recruitment in vascular lesions (Boring et al., 1998; Gu et al., 1998). The potent suppressive action of PPARγ and retinoid X receptor ligands on MCP-1-induced migration of THP-1 observed in our study suggests therefore the protective role of PPARγ in the development of atherosclerosis.

We also investigated in vivo the therapeutic effectiveness of troglitazone on acute recruitment of monocytes/macrophages onto the atheromatous lesion after balloon injury in WHHL rabbits. Since we utilized 10-month-old WHHL rabbits with fully developed atherosclerosis to examine the effect of troglitazone on the acute recruitment of monocytes onto atheromatous lesions, the effect of troglitazone on pre-existing atheromas was not as prominent as that reported by another study, which examined the effect of troglitazone on the development of atherosclerosis in younger WHHL rabbits (Shiomi et al., 1999). However, compatible with the in vitro effect of thiazolidinediones on monocytes/macrophages observed in our study, we also found in vivo evidence of suppression of acute adhesion and/or subsequent transendothelial migration in response to troglitazone treatment. Han et al. (2000) recently showed that oxLDL reduces circulating monocyte CCR2 expression through activation of PPARγ and postulated that oxLDL may promote the arrest of newly recruited monocytes in the arterial wall. However, our findings contradict their hypothesis, that is, the administration of the PPARγ agonist suppressed attachment and/or proliferation of monocytes/macrophages on atherosclerotic lesions at the site of balloon injury.

A previous study of ours found that thiazolidinediones stimulate endothelial proliferation and induce regeneration in vitro within clinically relevant doses (Fukunaga et al., 2001). The significant acceleration of re-endothelialization in the aorta after balloon injury observed in the study presented here was thus highly compatible with our previous in vitro findings. Accelerated re-endothelialization may be ascribed to the enhanced expression of pro-angiogenic factors previously demonstrated by us (Inoue et al., 2001; Itoh et al., 1999). In fact, troglitazone administration used in the current study showed increased gene expression of VEGF in the aorta of the WHHL rabbits.

In conclusion, we showed that PPARγ and retinoid X receptor specific ligands inhibited proliferation and migration of monocytes/macrophages as well as suppressed the functional expression of the MCP-1 receptor, CCR2 in THP-1. The administration of thiazolidinediones to WHHL rabbits inhibited monocyte/macrophage recruitment and induced endothelial regeneration after balloon injury. These results indicate the involvement of PPARγ in modulating monocyte proliferation, recruitment and transmigration through the endothelial cell layers under various pathological conditions and suggest the therapeutic potential of thiazolidinediones for diabetic vascular complications, which has been implied by some human studies (Minamikawa et al., 1998).

Acknowledgements

This work was supported in part by research grants from the Japanese Ministry of Education, Science and Culture, the Japanese Society for the Promotion of Science's 'Research for the Future' program (JSPS-RFTF 96100204, JSPS-RFTF 98L00801), and the Japan Smoking Research Foundation.

References

Boring, L., Gosling, J., Chensue, S.W., Kunkel, S.L., Farese Jr., R.V., Broxmeyer, H.E., Charo, I.F., 1997. Impaired monocyte migration and reduced type 1 (Th1) cytokine responses in C-C chemokine receptor 2 knockout mice. J. Clin. Invest. 100, 2552–2561.

Boring, L., Gosling, J., Cleary, M., Charo, I.F., 1998. Decreased lesion formation in CCR2–/– mice reveals a role for chemokines in the initiation of atherosclerosis. Nature 394, 894–897.

Charo, I.F., Myers, S.J., Herman, A., Franci, C., Connolly, A.J., Coughlin, S.R., 1994. Molecular cloning and functional expression of two monocyte chemoattractant protein-1 receptors reveals alternative splicing of the carboxyl-terminal tails. Proc. Natl. Acad. Sci. U. S. A. 191, 2752–2756.

Chen, Z., Ishibashi, S., Perrey, S., Osuga, J., Gotoda, T., Kitamine, T., Tamura, Y., Okazaki, H., Yahagi, N., Iizuka, Y., Shionoiri, F., Ohashi, K., Harada, K., Shimano, H., Nagai, R., Yamada, N., 2001. Troglitazone inhibits atherosclerosis in apolipoprotein E-knockout mice. Arterioscler. Thromb. Vasc. Biol. 21, 372–377.

Collins, A.R., Meehan, W.P., Kintscher, U., Jackson, S., Wakino, S., Noh, G., Palinski, W., Hsueh, W.A., Law, R.E., 2001. Troglitazone inhibits formation of early atherosclerotic lesions in diabetic and nondiabetic low density lipoprotein receptor-deficient mice. Arterioscler. Thromb. Vasc. Biol. 21, 365–371.

DeFronzo, R.A., Ferrannini, E., 1991. Insulin resistance: a multifaceted syndrome responsible for NIDDM, obesity, hypertension, dyslipidemia and atherosclerotic cardiovascular disease. Diabetes Care 14, 173–194.

Doi, K., Ikeda, T., Itoh, H., Ueyama, K., Hosoda, K., Ogawa, Y., Yamashita, J., Chun, T.-H., Inoue, M., Masatsugu, K., Sawada, N., Fukunaga, Y., Saito, T., Sone, M., Yamahara, K., Kook, H., Komeda, M., Ueda, M., Nakao, K., 2001. C-type natriuretic peptide induces redifferentiation of vascular smooth muscle cells with accelerated reendothelialization. Arterioscler. Thromb. Vasc. Biol. 21, 930–936.

Fukunaga, Y., Itoh, H., Doi, K., Tanaka, T., Yamashita, J., Chun, T.-H., Inoue, M., Masatsugu, K., Sawada, N., Saito, T., Hosoda, K., Kook, H., Ueda, M., Nakao, K., 2001. Thiazolidinediones, peroxisome proliferator-activated receptor γ agonists, regulate endothelial cell growth and secretion of vasoactive peptides. Atherosclerosis 158, 113–119.

Gu, L., Okada, Y., Clinton, S.K., Gerard, C., Sukhova, G.K., Libby, P., Rollins, B.J., 1998. Absence of monocyte chemoattractant protein-1 reduces atherosclerosis in low density lipoprotein receptor-deficient mice. Mol. Cell 2, 275–281.

Han, K.H., Chang, M.K., Boullier, A., Green, S.R., Li, A., Glass, C.K., Quenhenberger, O., 2000. Oxidized LDL reduces monocyte CCR2 expression through pathways involving peroxisome proliferator-activated receptor-γ. J. Clin. Invest. 106, 793–802.

Inoue, M., Itoh, H., Ueda, M., Naruko, T., Kojima, A., Komatsu, R., Doi, K., Ogawa, Y., Tamura, N., Takaya, K., Igaki, T., Yamashita, J., Chun, T.-H., Masatsugu, K., Becker, A.E., Nakao, K., 1998. Vascular endothelial growth factor (VEGF) expression in human coronary atherosclerotic lesions: possible pathophysiological significance of VEGF in progression of atherosclerosis. Circulation 98, 2108–2116.

Inoue, M., Itoh, H., Tanaka, T., Chun, T.-H., Doi, K., Fukunaga, Y., Sawada, N., Yamashita, J., Masatsugu, K., Saito, T., Sakaguchi, S., Sone, M., Yamahara, K., Yurugi, T., Nakao, K., 2001. Oxidized low density lipoprotein regulates VEGF expression in human macrophages and endothelial cells through activation of PPARγ. Arterioscler. Thromb. Vasc. Biol. 21, 560–566.

Itoh, H., Doi, K., Tanaka, T., Fukunaga, Y., Hosoda, K., Inoue, G., Nishimura, H., Yoshimasa, Y., Yamori, Y., Nakao, K., 1999. Hypertension and insulin resistance—the role of peroxisome proliferator-activated receptor-γ. Clin. Exp. Pharmacol. Physiol. 26, 558–560.

Kintscher, U., Goetze, S., Wakino, S., Kim, S., Nagpal, S., Chandraratna, R.A.S., Graf, K., Fleck, E., Hsueh, W.A., Law, R.E., 2000. Peroxisome proliferator-activated receptor and retinoid X receptor ligands inhibit monocyte chemotactic protein-1-directed migration of monocytes. Eur. J. Pharmacol. 401, 259–270.

Law, R.E., Meehan, W.P., Xi, X.-P., Graf, K., Wuthrich, D.A., Coats, W., Faxon, D., Hsueh, W.A., 1996. Troglitazone inhibits vascular smooth muscle cell growth and intimal hyperplasia. J. Clin. Invest. 98, 1897–1905.

Lehmann, J.M., Moore, L.B., Smith-Oliver, T.A., Wilkinson, W.O., Willson, T.M., Kliewer, S.A., 1995. An antidiabetic thiazolidinedione is a high affinity ligand for peroxisome proliferator-activated receptor gamma (PPAR gamma). J. Biol. Chem. 270, 12953–12956.

Minamikawa, J., Tanaka, S., Yamauchi, M., Inoue, D., Koshiyama, H., 1998. Potent inhibitory effect of troglitazone on carotid arterial wall thickness in type 2 diabetes. J. Clin. Endocrinol. Metab. 83, 1818–1820.

Nagy, L., Tontonoz, P., Alvarez, J.G.A., Chen, H., Evans, R.M., 1998. Oxidized LDL regulates macrophage gene expression through ligand activation of PPARgamma. Cell 93, 229–240.

Nelken, N.A., Coughlin, S.R., Gordon, D., Wilcox, J.N., 1991. Monocyte chemoattractant protein-1 in human atheromatous plaques. J. Clin. Invest. 88, 1121–1127.

Nolan, J.J., Ludvik, B., Beerdsen, P., Joyce, M., Olefsky, J., 1994. Improvement in glucose tolerance and insulin resistance in obese subjects treated with troglitazone. N. Engl. J. Med. 331, 1188–1193.

Ricote, M., Li, A.C., Willson, T.M., Kelly, C.J., Glass, C.K., 1998. The peroxisome proliferator-activated receptor-gamma is a negative regulator of macrophage activation. Nature 391, 79–82.

Sawada, N., Itoh, H., Ueyama, K., Yamashita, J., Doi, K., Chun, T.-H., Inoue, M., Masatsugu, K., Saito, T., Fukunaga, Y., Sakaguchi, S., Arai, H., Ohno, N., Komeda, M., Nakao, K., 2000. Inhibition of Rho-associated kinase results in suppression of neointimal formation of balloon-injured arteries. Circulation 101, 2030–2033.

Shiomi, M., Ito, T., Tsukada, T., Tsujita, Y., Horikoshi, H., 1999. Combination treatment with troglitazone, an insulin action enhancer, and pravastatin, an inhibitor of HMG-CoA reductase, shows a synergistic effect on atherosclerosis of WHHL rabbits. Atherosclerosis 142, 345–353.

Skorjanc, D., Jaschinski, F., Heine, G., Pette, D., 1998. Sequential increases in capillarization and mitochondrial enzymes in low-frequency-stimulated rabbit muscle. Am. J. Physiol. 274, C810–C818.

Tanaka, T., Itoh, H., Doi, K., Fukunaga, Y., Hosoda, K., Shintani, M., Yamashita, J., Chun, T.-H., Inoue, M., Masatsugu, K., Sawada, N., Saito, T., Inoue, G., Nishimura, H., Yoshimasa, Y., Nakao, K., 1999. Down regulation of peroxisome proliferator-activated receptor gamma expression by inflammatory cytokines and its reversal by thiazolidinediones. Diabetologia 42, 702–710.

Tontonoz, P., Hu, E., Spiegelman, B.M., 1994. Stimulation of adipogenesis in fibroblasts by PPAR gamma 2, a lipid-activated transcription factor. Cell 79, 1147–1156.

Tontonoz, P., Nagy, L., Alvarez, J.G.A., Thomazy, V.A., Evans, R.M., 1998. PPARgamma promotes monocyte/macrophage differentiation and uptake of oxidized LDL. Cell 93, 241–252.

Zhu, L., Bisgaier, C.L., Aviram, M., Newton, R.S., 1999. 9-*Cis* retinoic acid induces monocytes chemoattractant protein-1 secretion in human monocytic THP-1 cells. Arterioscler. Thromb. Vasc. Biol. 19, 2105–2111.

Available online at www.sciencedirect.com
SCIENCE DIRECT
Regulatory Peptides 127 (2005) 159–167
REGULATORY PEPTIDES
www.elsevier.com/locate/regpep

Angiotensin II suppresses growth arrest specific homeobox (Gax) expression via redox-sensitive mitogen-activated protein kinase (MAPK)

Takatoshi Saito[a], Hiroshi Itoh[a,*], Jun Yamashita[a], Kentaro Doi[a], Tae-Hwa Chun[a], Tokuji Tanaka[a], Mayumi Inoue[a], Ken Masatsugu[a], Yasutomo Fukunaga[a], Naoki Sawada[a], Satsuki Sakaguchi[a], Hiroshi Arai[a], Katsuyoshi Tojo[b], Naoko Tajima[b], Tatsuo Hosoya[c], Kazuwa Nakao[a]

[a]*Department of Medicine and Clinical Science, Kyoto University Graduate School of Medicine, 54 Shogoin Kawahara-cho, Sakyo-ku, Kyoto 606-8507, Japan*
[b]*Department of Internal Medicine, Division of Diabetes and Endocrinology, the Jikei University School of Medicine, Tokyo, Japan*
[c]*Department of Internal Medicine, Division of Nephrology and Hypertension, the Jikei University School of Medicine, Tokyo, Japan*

Received 2 May 2004; received in revised form 29 October 2004; accepted 18 November 2004
Available online 18 December 2004

Abstract

Oxidative stress is known to be involved in growth control of vascular smooth muscle cells (VSMCs). We and others have demonstrated that angiotensin II (Ang II) has an important role in vascular remodeling. Several reports suggested that VSMC growth induced by Ang II was elicited by oxidative stress. Gax, growth arrest-specific homeobox is a homeobox gene expressed in the cardiovascular system. Over expression of Gax is demonstrated to inhibit VSMC growth. We previously reported that Ang II down-regulated Gax expression. To address the regulatory mechanism of Gax, we investigated the significance of oxidative stress in Ang II-induced suppression of Gax expression. We further examined the involvement of mitogen-activated protein kinases (MAPKs), which is crucial for cell growth and has shown to be activated by oxidative stress, on the regulation of Gax expression by Ang II. Ang II markedly augmented intracellular H_2O_2 production which was decreased by pretreatment with *N*-acetylcystein (NAC), an anti-oxidant. Ang II and H_2O_2 decreased Gax expression dose-dependently and these effects were blocked by administration of both NAC and pyrrolidine dithiocarbamate (PDTC), another anti-oxidant. Ang II and H_2O_2 induced marked activation of extracellular signal-responsive kinase1/2 (ERK1/2), which was blocked by NAC. Ang II and H_2O_2 also activated p38MAPK, and they were blocked by pre-treatment with NAC. However, the level of activated p38MAPK was quite low in comparison with ERK1/2. Ang II- or H_2O_2-induced Gax down-regulation was significantly inhibited by PD98059, an ERK1/2 inhibitor but not SB203580, a p38MAPK inhibitor. The present results demonstrated the significance of regulation of Gax expression by redox-sensitive ERK1/2 activation.

Keywords: Angiotensin II; Gax; Mitogen-activated protein kinase; Vascular smooth muscle cell; Oxidative stress

1. Introduction

The physiological production of reactive oxygen species (ROS) such as superoxide (O2–) and hydrogen peroxide (H_2O_2) is necessary for maintenance of normal cell function and cell homeostasis, however, surplus generation of ROS called as oxidative stress has been implicated in pathophysiological mechanism [1,2]. In vasculature, growth of vascular smooth muscle cells (VSMCs) is shown to be elicited by oxidative stress [3,4]. In contrast, treatments with antioxidants such as *N*-acetylcystein (NAC) have been reported to inhibit cell growth in cultured VSMC [5]. In vivo, advanced glycation end-products and oxidized LDL which have been shown to induce atherosclerosis via VSMC growth and migration also promote oxidative stress through intracellular ROS generation [6,7]. Moreover, some types of hypertension and development of restenosis after angioplasty are shown to be incited by oxidative stress through VSMCs growth [8]. Thus, oxidative stress seems to play a consequent role in vascular diseases.

* Corresponding author. Tel.: +81 75 751 3170; fax: +81 75 771 9452.
E-mail address: hiito@kuhp.kyoto-u.ac.jp (H. Itoh).

0167-0115/$ - see front matter © 2004 Elsevier B.V. All rights reserved.
doi:10.1016/j.regpep.2004.11.006

We and others have demonstrated that angiotensin II (Ang II) has an important role in vascular remodeling [9,10]. Recently several reports have suggested that growth stimulation of VSMC and hypertension induced by Ang II was elicited with ROS generation. Laursen et al. demonstrated that Ang II-induced hypertension was produced by an increase in endogenous free radical generation and that chronic infusion of liposome-encapsulated superoxide dismutase (SOD), a specific reductase to O2–, markedly decreased blood pressure increase by Ang II [11]. Another report has also demonstrated that Ang II-induced increase in [3H] leucine incorporation in VSMC is remarkably inhibited by overexpression of catalase, a specific reductase that converts H_2O_2 to water and oxygen, suggesting that H_2O_2 generated with Ang II stimulation was a crucial signaling in vascular hypertrophy [12]. These observation all together indicate that redox-sensitive signaling pathway is an important component in Ang II-modulated vascular remodeling, however, the mechanism underlying these effects remains still unclear.

Homeobox genes implicated in gene transcription have a crucial role in cell proliferation and migration [13]. Growth arrest-specific homeobox (Gax) widely distributed in cardiovascular system [14]. It is reported that Gax expression is suppressed with growth stimulation induced by serum or platelet-derived growth factor (PDGF) in quiescent VSMCs [14]. Microinjection of a recombinant Gax protein or overexpression of Gax by infection with an adenovirus Gax construct induces inhibition of G0/G1 cell cycle transition in a p21cip1-dependent manner in vitro and reduced vessel stenosis in a rabbit model of balloon angioplasty [15,16]. We and others revealed that vasoactive substances especially occurring within the blood vessels not only regulate vascular tone but also modulate vascular growth [17]. Vasoconstrictive peptides such as Ang II and endothelin promote vascular growth and, conversely, vasodilating substances such as natriuretic peptides (NPs) and nitric oxide inhibit vascular growth [3,18,19]. We recently demonstrated that Ang II and NPs oppositely regulate Gax expression in VSMCs [20]. However, the mechanism of the Gax regulation pathway has not been established. To address the regulation mechanism of Gax expression, we investigated the significance of ROS in Ang II-induced suppression of Gax expression. In addition, we further examined the involvement of mitogen-activated protein kinases (MAPKs), which are crucial for cell growth and have shown to be activated by ROS, in regulation of Gax expression by Ang II.

2. Material and method

2.1. Reagents

Human Ang II was purchased from Peptide Institute (Osaka, Japan). Dimethyl sulfoxide (DMSO) and NAC were obtained from *Nacalai tesque* (Kyoto, Japan). [α32-P] dCTP (3000 Ci/mmol) was obtained from Amersham International (Aylesbury, UK). PD98059, an inhibitor of extracellular signal-responsive kinase 1 and 2 (ERK1/2) kinase inhibitor, and SB203580, an inhibitor of p38MAPK, and pyrrolidine dithiocarbamate (PDTC) were obtained from Sigma (St. Louis, MO).

2.2. Cell culture

Aortic VSMCs harvested from male Wistar rats were purchased from TOYOBO and were grown in Dulbecco's modified Eagle's medium (DMEM, Nikken Bio Medical Laboratories, Tokyo, Japan) supplemented with 10% fetal calf serum (FCS, Cell culture Laboratories, Cleveland, OH, U.S.A.) with 100 U/mL penicillin and 100 μg/mL streptomycin. Cells were maintained at 37 °C in a humidified atmosphere of 95% air–5% CO_2. VSMCs from 4th to 8th passage were used in the present study.

2.3. Intracellular H_2O_2 measurement

VSMCs were plated into 10-cm-diameter dishes and grown up to about 60–80% confluent in culture medium containing 10% FCS, and made quiescent by additional 24 h in FCS free DMEM. Then, the medium was replaced with fresh DMEM and incubated for 30 min with or without NAC and for 10 min with 10 μM H_2O_2-sensitive fluorophore 2′, 7′-dichlorofluorescin diacetate (DCF-DA, Sigma) before 100 nM Ang II or 200 μM H_2O_2 treatment. Cells were stimulated with H_2O_2 or Ang II for 5 min and washed 2 times with ice-cold PBS and placed on ice. Cells were harvested with 1 mL Trypsin/EDTA and centrifuged at 2000×*g* in a microcentifuge [4] for 5 min. Cells were washed twice with ice-cold PBS and resuspended with 0.4 mL ice-cold PBS. The levels of intracellular H_2O_2 were measured by FACS Caliber (Becton Dickinson) as described elsewhere [21].

2.4. RNA preparation and Northern blot analysis

VSMCs were plated and quiescent as described above for estimation of Gax mRNA expression. Cells were pre-treated with 1 mM NAC, 50–500 μM PDTC, 30 μM PD98059, and 10 μM SB203580 or vehicle for 30 min in case of need and stimulated with various concentration of AngII and H_2O_2. Cells were incubated for 6 h and harvested for RNA isolation. Total cellular RNA extraction and estimation of Gax mRNA expression were performed as previously reported [20].

2.5. Detection of ERK1/2 phosphorylation by immunobloting

VSMCs were plated and quiescent as described above for estimation of ERK1/2 phosphorylation by immunobloting.

Cells were stimulated with 100 nM Ang II and 200 μM H_2O_2 for various times with or without pre-treatment of NAC for 30 min. After treatment, cells were washed twice with ice-cold PBS and placed on ice immediately. Cells were lysed with 100 μL SDS sample buffer (50 mM Tris–HCl, 100 mM DTT, 2% SDS, 0.1% BPB, 10% glycerol). Solubilized proteins were quantified by the Lawry method using protein assay kit (Bio-Lad). Proteins (25 μg) were separated on 12.5% polyacrylamide gels using SDS–PAGE and transferred to nitrocellulose membrane at 40 mA for 57 min. Membranes were blocked overnight at 4 with TBS-T containing 5% non-fat dry milk and 0.1% Tween 20. The blots were incubated for overnight at 4 °C with primary antibody (rabbit polyclonal anti-phospho specific ERK1/2 antibody at 1:1000, New England Biolabs; NEB, Boverly, MA) in TBS-T and incubated for 1 h at room temperature with secondary antibody (AP-conjugated gout anti-rabbit antibody at 1:1000, NEB) in same buffer. Phospholylated ERK1 and 2 were visualized with NBT/BCIP solution (Boehringer Mannheim).

2.6. Immunoprecipitation and p38MAPK activity assay

VSMCs were plated and quiescent as described above for estimation of p38MAPK activity assay. Cells were stimulated with agonists at 37 °C in serum free DMEM for specified durations. After treatment, cells were washed twice with ice-cold PBS and placed on ice. Cells were lysed with ice-cold buffer containing 20 mM Tris–HCl pH 7.5, 150 mM NaCl, 1 mM EDTA, 1 mM EGTA, 1% Triton X-100, 2.5 mM sodium pyrophosphate, 1 mM β-glycerolphosphate, 1 mM Na_3VO4, 1 μg/mL leupeptin, protease inhibitor cocktail (Sigma) and sonicated 4 times for 5 s each, on ice. Cell lysates were then centrifuged at 13000×*g* for 10 min at 4 °C. For immunoprecipitation, 300 μg cell lysates was incubated with anti-p38MAPK antibody (1:50) for overnight at 4 °C with gentle rocking, and then 20 μL of protein G-sepharose beads added and incubated for 3 h at 4 °C with gentle rocking. The beads were washed twice with 500 μL of cell lysis buffer and twice with 500 μL of kinase buffer (25 mM Tris–HCl pH 7.5, 5 mM β-glycerolphosphate, 2 mM DTT, 0.1 mM Na_1VO4, 10 mM MgCl2). For kinase assay, the beads were suspended with 50 μL of kinase buffer supplemented with 200 μM ATP and 2 μg ATF-2 fusion protein, the substrate for p38MAPK, and incubated 30 min at 30 °C. Proteins were separated on 12.5% polyacrylamide gels using SDS–PAGE and transferred to nitrocellulose membrane at 40 mA for 57 min. Membranes were locked overnight at 4 °C with TBS-T. The blots were incubated for overnight at 4 °C with primary antibody (rabbit polyclonal anti-ATF-2 antibody at 1:1000, NEB) in TBS-T and incubated for 1 h at room temperature with secondary antibody (HRP-conjugated gout anti-rabbit antibody at 1:2000, NEB) in same buffer. Phospholylated ATF-2 protein was detected with ECL solution.

2.7. Statistical analysis

All results were expressed as mean±S.D. Statistical analysis of the data was performed using ANOVA. $P<0.05$ was considered to be statistically significant.

3. Results

3.1. Effect of exogenous H_2O_2 and Ang II on intracellular H_2O_2 level

To address the effect of H_2O_2 and Ang II on intracellular H_2O_2 accumulation in VSMCs, we exposed cells to 200 μM H_2O_2 or 100 nM Ang II for 5 min and measured the concentration of DCFH-DA oxidized by H_2O_2 per 1×10^4 cells. Fig. 1 shows H_2O_2- or Ang II-induced representative

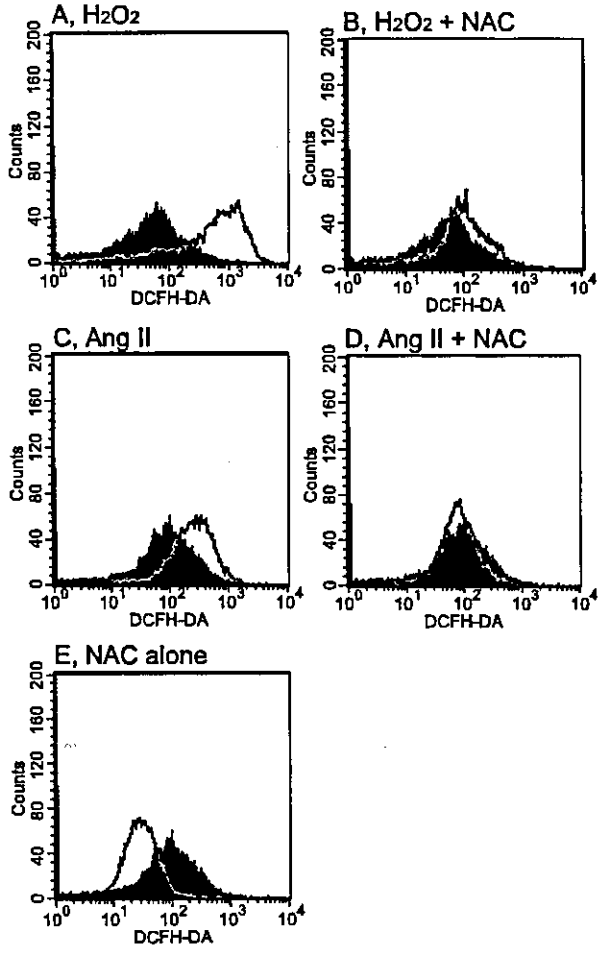

Fig. 1. Change of intracellular H_2O_2 level by Ang II and H_2O_2 treatment in VSMCs. Quiescent VSMCs pretreated with DCF-DA for 10 min were stimulated by 200 M H_2O_2 (A, B), 100 nM Ang II (C, D) or vehicle (E) for 5 min with (B, D, E) or without (A, C) 1 mM NAC pretreatment for 30 min. Then, cells were lysed with Tripsin/EDTA, washed twice with ice-cold PBS and resuspended with ice-cold PBS. The fluorescence intensity of 1×10^4 cells was analysed using a Becton Dickinson FACScan. The experiments were repeated at least two times with similar results.

alteration of intracellular H_2O_2 level in VSMCs as measured by flow cytemetry. As shown in Fig. 1A, exogenous H_2O_2 200 μM remarkably shifted the peak of DCF fluorescence intensity to the right. These effects were almost completely blocked by pre-treatment with 1 mM NAC for 30 min (Fig. 1B). 100 nM Ang II also increased in H_2O_2 concentration (Fig. 1C). Pre-treatment with 1 mM NAC completely inhibited H_2O_2 production by Ang II stimulation (Fig. 1D). Treatment with NAC alone reduced basal production of H_2O_2 (Fig. 1E).

3.2. Effect of Ang II and H_2O_2 on Gax mRNA expression

To determine whether the down-regulation of Gax mRNA expression with Ang II, which we previously reported, is required for oxidative stress, the effect of Ang

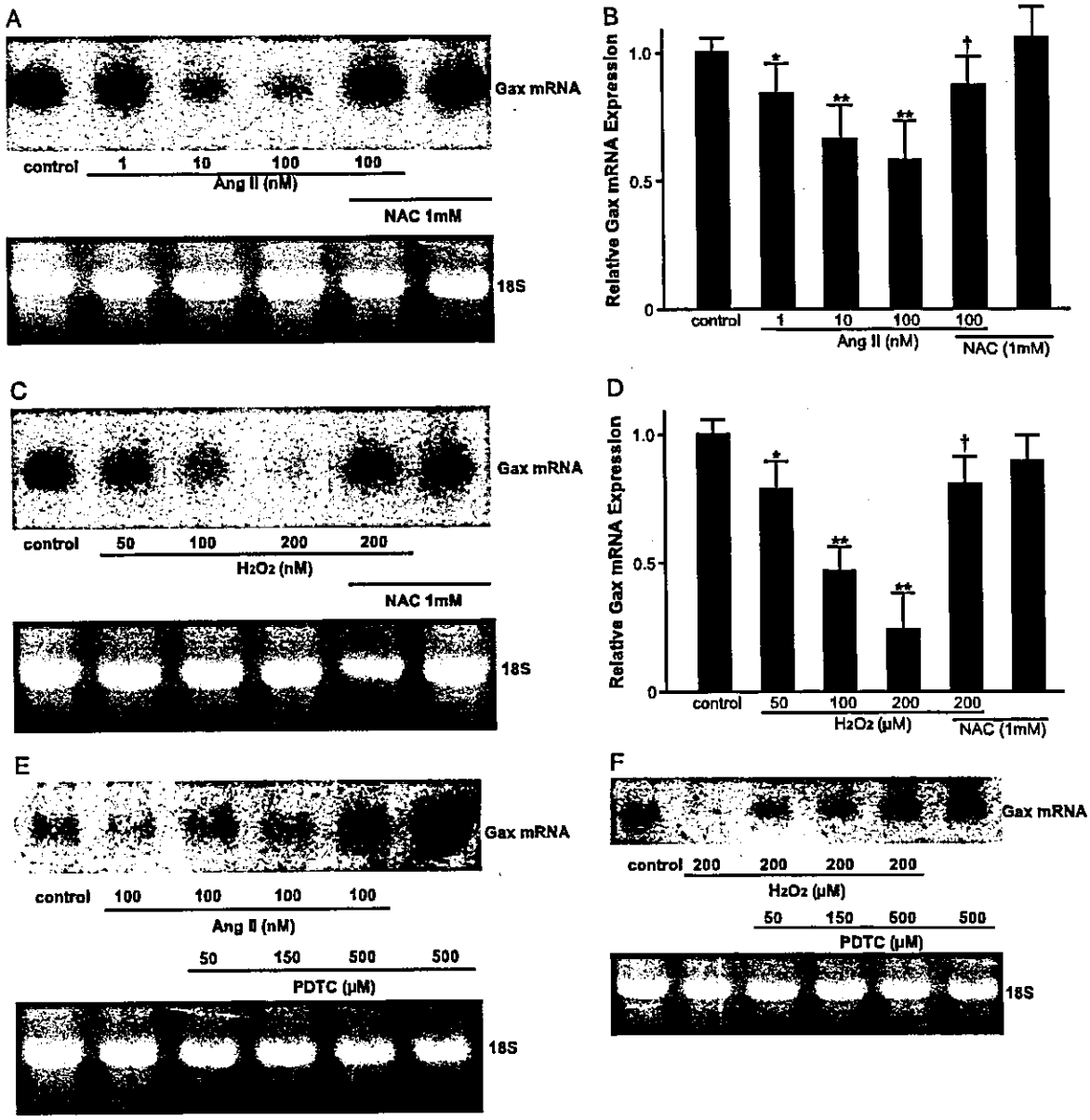

Fig. 2. Dose-dependent effect of Ang II or H_2O_2 on Gax mRNA expression with or without pretreatment of NAC for 30 min. Dose-dependent effect of PDTC on Ang II- or H_2O_2-induced down-regulation of Gax mRNA. (A, C, E, and F) Northern blot analysis for Gax mRNA expression. Quiescent VSMCs were stimulated by vehicle or various concentrations of Ang II for 6 h with or without pretreatment of NAC or PDTC for 30 min and then harvested. Equal aliquots of total RNA (25 g) per lane were applied for the analysis. Lower panel depicts the images of 18S. (B and D) Quantitative measurements of Gax mRNA levels stimulated by Ang II or H_2O_2. The data represent the average percentage of the control. Bars represent the mean±S.D. (n=3). P<0.05, P<0.01 vs. control cells. P<0.05 vs. 100 nM Ang II or 200 M H_2O_2 alone. The experiments for the effects of NAC and PDTC were repeated three times and (n=2 on each), and similar results were obtained.

II and H_2O_2 in the presence or absence of NAC on Gax mRNA expression was examined. As shown in Fig. 2A and B, the administration of Ang II suppressed Gax mRNA expression in a dose-dependent manner. 100 nM Ang II suppressed Gax mRNA expression by about 50% compared with control. The down-regulation of Gax mRNA induced by Ang II was significantly blocked with 1 mM NAC. As shown in Fig. 2C and D, H_2O_2 also suppressed Gax mRNA expression dose-dependently and 200 μM H_2O_2 down-regulated Gax mRNA expression by about 80% compared with control. Pre-treatment with NAC markedly inhibited the down-regulation of Gax mRNA expression induced by H_2O_2. NAC alone has no significant effect on Gax mRNA expression. Moreover, we investigated effects of another antioxidant, PDTC on Ang II- and H_2O_2-induced down-regulation of Gax mRNA in order to delineate the significance of redox-sensitive cascade further. Down-regulation of Gax mRNA expression elicited by Ang II or H_2O_2 was abrogated by PDTC dose-dependently as shown in Fig. 2E and F.

3.3. Effect of Ang II and H_2O_2 on MAPKs phosphorylation

To determine whether the activation of MAPKs induced by Ang II is redox-sensitive or not, we examined the effect of Ang II and H_2O_2 on activation of ERK1/2 and p38MAPK in VSMCs with or without NAC. Fig. 3A shows the time-course of the effect of 100 nM Ang II on ERK1/2 phosphorylation. Rapid and transient phosphorylation of ERK1/2 observed after Ang II stimulation occurred within 5 min and declined 10–30 min after. Pre-treatment with 1 mM NAC potently decreased ERK1/2 phosphorylation elicited with Ang II at 5 min. As shown in Fig. 3B, treatment of 200 μM H_2O_2 also increased ERK1/2 phosphorylation and its activation peaked at 15–20 min and declined in 20–30 min. Pre-treatment of 1 mM NAC also markedly down-regulated H_2O_2-induced ERK1/2 phosphorylation at 20 min similarly.

We also examined the effect of Ang II and H_2O_2 on p38MAPK tyrosine phosphorylation in VSMCs. We could not detect significant phosphorylation of p38MAPK by using the method similar to ERK1/2 measurement. Therefore, we further measured p38MAPK activity using immunoprecipitation (Fig. 3C and D). Ang II and H_2O_2 also slightly activated p38MAPK, and they were blocked by pre-treatment with NAC. However, the level of activated p38MAPK was quite low in comparison with ERK1/2.

3.4. Effect of PD98059 and SB203580 on Ang II-induced down-regulation of Gax mRNA expression

The results presented above demonstrated that Ang II triggered ERK1/2 activation through redox-sensitive signaling in VSMCs. To address the relation of the redox-sensitive MAPK to oxidative stress-induced down-regulation of Gax mRNA expression, we examined the effect of PD98059 and SB203580 on Ang II-induced down-regulation of Gax

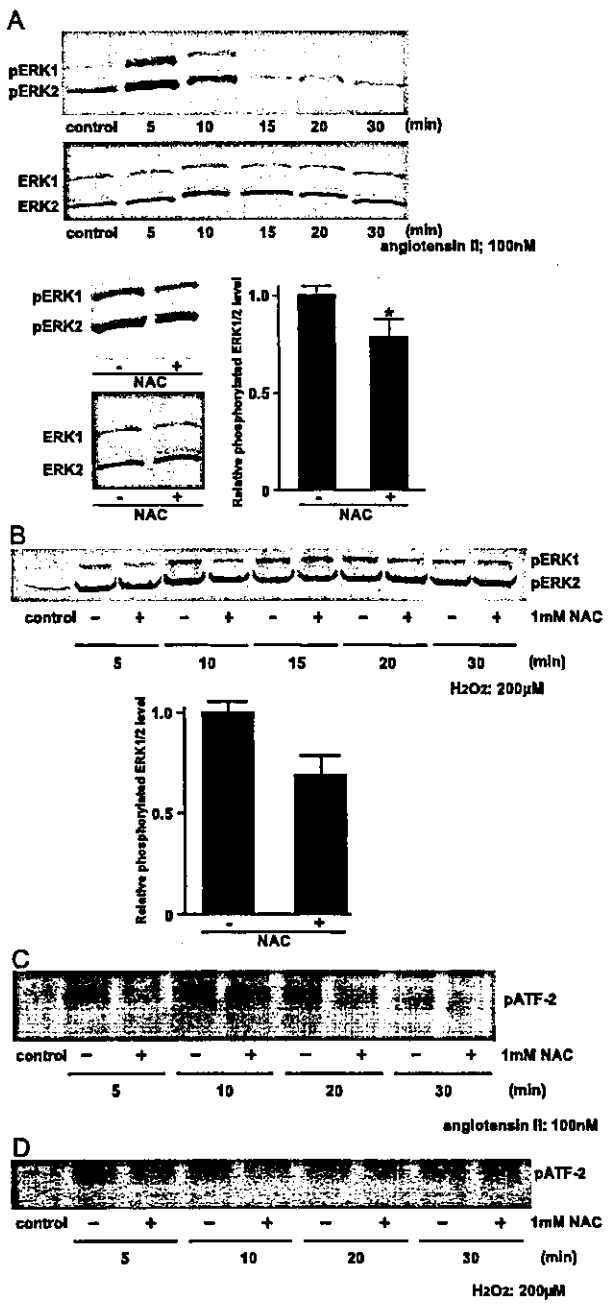

Fig. 3. Effect of Ang II (A) or H_2O_2 (B) on ERK1/2 phosphorylation and effect of NAC on phosphorylated ERK1/2 induced by Ang II or H_2O_2. Quiescent VSMCs were stimulated by 100 nM Ang II or 200 M H_2O_2, respectively, for different time points. NAC was pre-treated for 30 min before administration of Ang II or H_2O_2. Equal aliquots of protein (25 g) from the VSMC lysate were separated by 12.5% SDS–PAGE, followed by immunoblotting for phosphorylated ERK1/2 (pERK1, pERK2). Parallel blots were assayed using the antibodies recognizing the total ERK proteins (ERK1, ERK2). Upper panel represents time-course of ERK1/2 phosphorylation by Ang II or H_2O_2 with or without NAC. Lower panels shows the effect of NAC on the peak level of ERK1/2 phosphorylation induced by Ang II (5 min) or H_2O_2 (20 min). $P<0.01$ vs. control cells. The experiments were repeated four times with similar results. Effect of Ang II (C) or H_2O_2 (D) on ATF-2 phosphorylation and effect of NAC on phosphorylated ATF-2 induced by Ang II or H_2O_2.

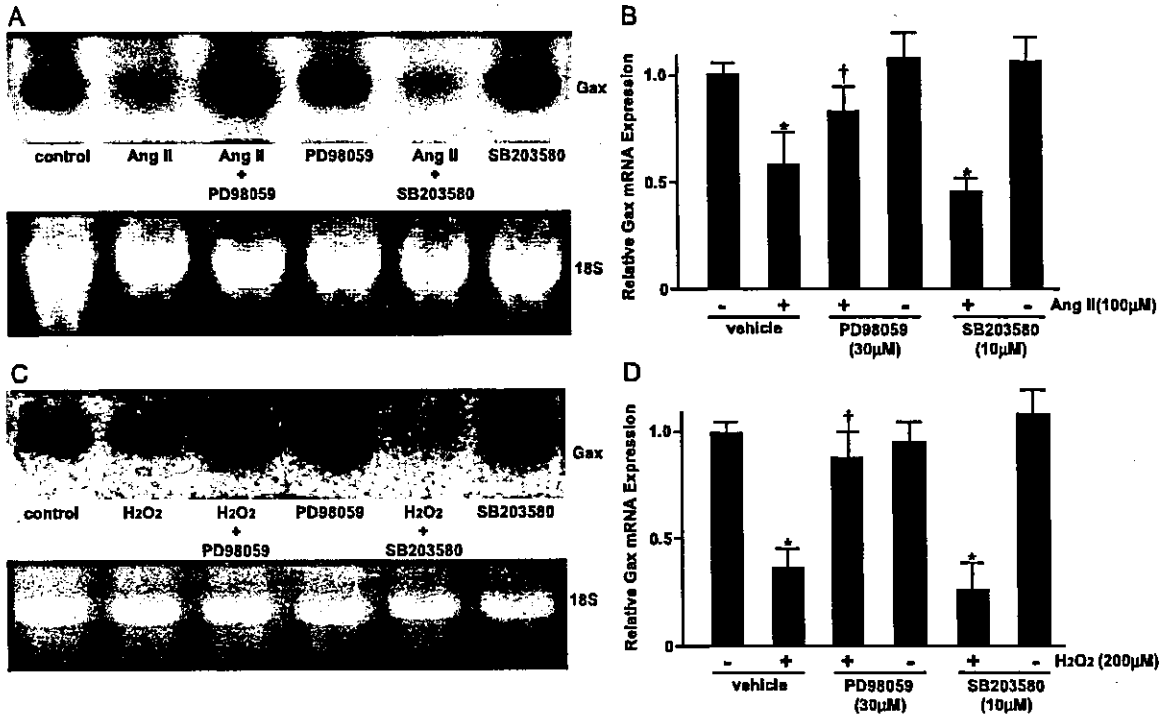

Fig. 4. Effect of PD98059 or SB203580 on Ang II-induced suppression of Gax mRNA expression. (A and C) Northern blot analysis for Gax mRNA expression. Quiescent VSMCs were stimulated by 100 nM Ang II or 200 M H_2O_2 for 6 h with or without pretreatment of PD98059 or SB203580 for 30 min, and then harvested. Equal aliquots of total RNA (25 g) per lane were applied for the analysis. (B and D) Quantitative measurements of Gax mRNA levels stimulated by Ang II or H_2O_2. Bars represent the mean S.D. (n=3). P<0.05, P<0.01 vs. control cells. P<0.05 vs. 100 nM Ang II or 200 M H_2O_2 alone. The experiments were repeated at least three times with similar results.

mRNA expression. As shown in Fig. 4A and B, pretreatment with PD98059 significantly inhibited Ang II-induced down-regulation of Gax mRNA expression by 80% compared with control, while the administration of SB203580 had no effect on Gax expression 6 h after Ang II stimulation. Similarly, PD98059 significantly inhibited H_2O_2-induced down-regulation of Gax mRNA, whereas SB203580 exerted no significant effect.

4. Discussion

In the present study, we demonstrated that Ang II increased intracellular H_2O_2 level and suppressed Gax expression. H_2O_2 mimicked suppressive effect of Ang II on Gax expression. Both Ang II- and H_2O_2-induced down-regulation of Gax expression were blocked by NAC and PDTC. These data indicated that Ang II suppressed Gax expression via increase in intracellular H_2O_2 level. Previously, we reported that down-regulation of Gax expression by Ang II was completely abolished by pretreatment with Ang II type 1 receptor (AT1-R) antagonist, CV11974 [20]. Zafari et al. suggested that Ang II-induced increase in H_2O_2 was inhibited by AT1-R antagonist, losartan [22]. These findings suggest that both the down-regulation of Gax expression and H_2O_2 generation caused by Ang II stimulation were triggered via signaling cascade from AT1-R and imply that H_2O_2 generation mediated via AT1-R activation is involved in Ang II-induced down-regulation of Gax.

It has been reported that Ang II activates three MAPKs, ERK1/2, the c-*jun* NH2-terminal kinases (JNKs, also termed stress-activated protein kinase, SAPK), and p38MAPK in VSMCs [23]. ERK1/2 is rapidly activated in response to virtually all growth factors, leading to a rapid increase in expression of the growth-associated nuclear proto-oncogenes, c-*fos*, c-*jun*, and c-*myc* and recognized to be essential for control of cell growth, division and differentiation in various cells. In contrast, JNK and p38 MAPK are recognized to be activated by environmental stress such as ultraviolet, lipopolysaccharide, hypoxia, osmotic stress, heat shock, and inflammatory cytokines. Recent reports have shown that ERK1/2 and p38MAPK are activated by ROS in VSMCs [12,24]. Therefore, we examined the possible involvement of MAPKs in down-regulation of Gax expression by Ang II or H_2O_2. Both Ang II and H_2O_2 markedly activated ERK1/2 but did not induce p38MAPK phosphorylation significantly. Moreover, down-regulation of Gax by Ang II or H_2O_2 was significantly abrogated by PD98059 administration, while pretreatment with SB203580 had no effect on Gax expression. These results suggest that Ang II or H_2O_2 induce ERK1/2 activation, and down-regulate Gax expression mainly through ERK1/2 activation, indicating that redox-sensitive

ERK1/2 activation is involved in the signaling cascade of Ang II–Gax pathway.

In this study, we demonstrated that Ang II increased in intracellular H_2O_2 concentration within 5 min. As shown in Fig. 3A, in Ang II-induced ERK1/2 activation, the pathway via elevation of intracellular H_2O_2 concentration is considered to exert the effect 5 min after Ang II administration. As for Ang II-induced down-regulation of Gax mRNA as shown in Fig. 4, the pathway via ERK1/2 activation contributed to it by about 50%. In contrast, as shown in Fig. 4D, H_2O_2 suppresses Gax mRNA expression mainly via ERK1/2 activation. Therefore, other pathways besides H_2O_2 pathways are responsible for Ang II-induced down-regulation of Gax mRNA expression.

We demonstrated the transient and rapid phosphorylation of ERK1/2 and increment of H_2O_2 concentration induced by Ang II within 5 min. Moreover, we also showed that slow activation of ERK1/2 in spite of rapid increment of intracellular H_2O_2 concentration induced by exogenous H_2O_2 administration. This discrepancy may suggest that H_2O_2 has a minor role for the peak of Ang II-induced ERK1/2 phospholylation within 5 min, and increment of intracellular H_2O_2 is more related to the late phase of ERK1/2 phospholylation (Fig. 3B). Eguchi and colleagues demonstrated that Ang II-induced MAPK activation could be mediated by p21ras activation through a currently unidentified tyrosine kinase that lies downstream of Gq-coupled Ca2+/calmodulin signals [25]. In fact, as shown in Fig. 3A and B, NAC-induced suppression of ERK1/2 phospholylation was only 20%. We considered that Ang II induced ERK1/2 phospholylation through several signal transductions perhaps including the increment of intracellular H_2O_2 concentration.

Baas et al. demonstrated that Ang II produces superoxide in VSMCs [26]. In the present study, superoxide was certainly produced and would contribute to the results we showed. Superoxide is commonly known to be reduced by superoxide dismutase to H_2O_2, therefore, we consider that Ang II increases intracellular H_2O_2 concentration through superoxide production and causes the effects. Although we did not investigate a specific effect of superoxide, we believe that could sufficiently demonstrate the function of Ang II-induced oxidative stress by examining the effects of H_2O_2 as a metabolite of superoxide and NAC as an antioxidant agent.

Both Ushio-Fukai et al. and Zafari et al. previously showed that oxidative stress rapidly induced by Ang II administration was important for VSMCs growth [12,22,27]. Several reports revealed that suppression of Gax expression was related to growth retardation of VSMCs [14,15,20]. As mentioned above, the present study also supports that oxidative stress induces growth of VSMCs possibly in part via suppression of Gax expression. Ushio-Fukai et al. have shown that only p38MAPK, but not ERK1/2, is activated by H_2O_2 in VSMC and involved in Ang II-induced VSMC hypertrophy [12]. In our study, Ang II induced marked ERK1/2 activation but did not cause significant augmentation of p38MAPK activity, and the former is crucial for down-regulation of Gax expression, although exact reason for the difference is unclear at present, there might be the possibility that the culture condition of the cells is different. The passage and culture medium were identical. When the cells were made quiescent, we performed the experiments without serum, while they did the experiment with 0.1% serum. Furthermore, whereas they administrated agents under the conditions of 80–90% cell density, we performed the experiments with 50–70% cell density.

Recently, Abe et al. have showed that H_2O_2 activates ERK1/2 dose-dependently in bovine tracheal smooth muscle cells [28]. Lee et al. also showed H_2O_2 activated ERK1/2 in a time-dependent fashion in rat lung artery smooth muscle cells and activation of ERK1/2 reached maximal level 20 min later [29]. Moreover, Frank et al. revealed that H_2O_2 induced ERK1/2 activation in VSMCs [30]. These results are compatible with our results. On the other hand, Huot et al. showed that p38MAPK was induced by H_2O_2 [31]. The difference on Ang II-induced p38MAPK is not clear at present.

Previously, Tsai et al. showed NAC and PDTC induce apoptosis in VSMCs [32]. They demonstrated the results using 5 mM NAC, which was considered to be very high. In addition, their experiments were performed in very low cell density condition. It is considered that apoptosis was easily induced in their experimental condition. As mentioned above, we performed all experiments in higher cell density condition compared to their experiments. We did not confirm whether apoptosis was induced by NAC administration, however, we consider that there is little involvement of apoptosis in the present study, since floating cells were not seen in NAC-treated groups and there was no difference in the time amount of RNA harvested from VSMCs with NAC-treated groups and non-treated groups.

In our previous report, we speculated that gene regulation of Gax expression was under control of a molecule commonly used by AT1-R and PDGF receptor signaling pathways because of the similar action of Ang II and PDGF on Gax expression [20]. In this study, it was shown that down-regulation of Gax by Ang II is mediated through redox-sensitive ERK1/2 activation. In another series of our experiment, we have confirmed that PDGF-induced down-regulation of Gax is also remarkably suppressed by treatment with NAC. These findings suggests the existence of redox-sensitive pathway, which induces down-regulation of Gax, after the convergence of AT1-R and PDGF receptor signaling pathways. Sundaresan et al. exhibited that the PDGF-stimulated increase in intracellular H_2O_2 and the effects of PDGF stimulation on ERK1/2 activation, migration, and DNA synthesis were inhibited by infection of VSMCs with an adenovirus that encodes catalase, a specific reductase of H_2O_2 [33]. These evidences and our data indicate the significance of intracellular H_2O_2 accumulation and ERK1/